

ANALYSIS OF THE PERIODIC SPECTRAL GAPS OBSERVED IN THE TUNING RANGE OF FELS WITH A PARTIAL WAVEGUIDE

R. Prazeres, F. Glotin, J.-M. Ortega, LCP / CLIO, Université de Paris Sud, ORSAY, FRANCE

Abstract

A phenomenon of “Spectral Gaps“ is observed in far-infrared FELs using partial waveguiding : the laser power falls down to zero at some particular wavelengths, whatever the beam adjustments are. We show that this effect is related to a periodic increase of the cavity losses, with a period depending on the dimensions of the waveguide. A numerical code including diffraction effects exhibits good agreement with the measurements.

INTRODUCTION

Several infrared Free-Electron Lasers (FEL) are presently used around the world as light sources by a large scientific community [1]. FELs are especially efficient in infrared since they produce high power laser pulses, and are tunable across a large wavelength range, typically 1 to 2 decades. The CLIO FEL [2] [3] spans from $3\mu\text{m}$ to $150\mu\text{m}$, obtained by varying the beam energy from 50 to 12 MeV. This is the largest tuning range obtained with a single beam line. However, as the wavelength increases, the diffraction limited optical mode transverse size tends to undergo losses at the undulator vacuum chamber (Fig.1). The size of this chamber cannot be increased if one wants to maintain a sufficiently strong undulator magnetic field on-axis. Therefore, several FELs [4] [5] have designed the vacuum chamber so as to use it as an optical waveguide in the direction parallel to the magnetic field. In this configuration, detailed measurements of FEL power at large wavelength exhibit a phenomenon of Spectral Gap : for example, at $\lambda=45\mu\text{m}$ the CLIO FEL power falls down to zero or vanishes strongly. This effect is always present, independently of electron beam tunings or of cavity mirror radius of curvature. This phenomenon is also observed in other infrared FELs, which are working in the same configuration : FELIX [4] and ELBE [5].

In order to provide an explanation for these Spectral Gaps, we have developed an in-house numerical code [6] [7] [8] which calculates the cavity losses, the intracavity laser power of the FEL and the output laser power. This code takes into account the configuration of the optical cavity for the partially waveguided FEL with hole extraction. Finally, we show that a simple analytical calculation of the phase advance of light in the waveguide account for the periodic behaviour of this Spectral gap.

OPTICAL CAVITY

The optical cavity of a FEL is always several meters long, because it includes enough space for the undulator

and for the magnetic elements used to drive the electron beam. As an example, the layout of the CLIO FEL is displayed on figure 1. The distance between cavity mirrors is 4.8 meters. The vertical inner size of vacuum chamber is limited to 14 mm, in order to allow wavelength tuning by the undulator gap. The horizontal size is 35 mm. In first approximation, the elliptical shape of cross section of the waveguide allows one to consider the waveguide as a pair of infinite parallel plates, as shown in figure 1. A waveguide is created by using an undulator vacuum chamber of good optical quality. This is realized by using extruded aluminium which possesses a good conductivity and reflectivity.

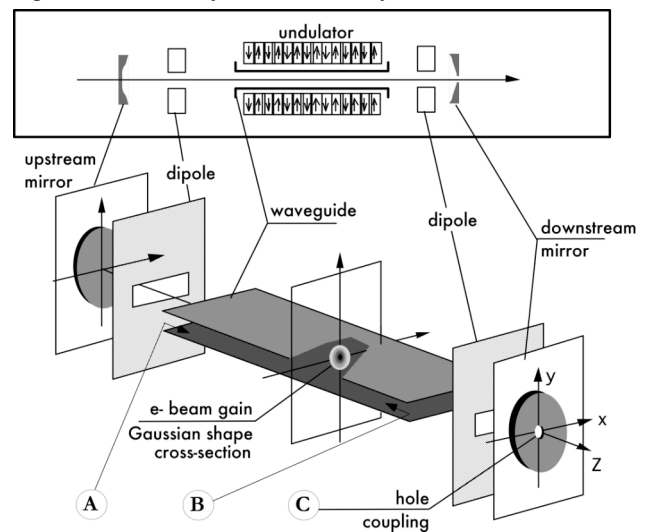


Figure 1: Schematic layout of the CLIO Free-Electron Laser optical cavity.

Therefore, optical guiding only occurs along one axis corresponding to the minimum waveguide dimension (vertical axis in figure 1), whereas wave propagation is free along the other axis (horizontal in figure 1). Also, the waveguide length does not fill the whole space of the cavity : The area close to the mirrors is in “free propagation mode“. This hybrid configuration induces a “partial guiding“ of the laser mode. At short wavelength ($\lambda < 10\mu\text{m}$) the waveguide does not modify the laser mode, because it is larger than its dimensions. The Gaussian beam propagation analytical theory is then valid. However, at large wavelength (typically $\lambda > 50\mu\text{m}$) the laser mode becomes guided in the vacuum chamber, and remains free propagating elsewhere. In the intermediate regime, the mode is partially guided in the extremities of the waveguide.

Another feature of the cavity can be responsible of important perturbations of the laser mode : the output coupling is performed by a hole of 2 or 3 mm in the center of one cavity mirror. This solutions is advantageous as compared to using a beam splitter because it does not create optical absorption, specially at large wavelength where transparent materials are rare and of poor optical quality. However, the output coupling factor of the hole, i.e. ratio between output power and intra-cavity power, is strongly dependant on the transverse distribution of the laser mode at the output mirror.

A less important feature must still be considered here, which is typical of the FEL process, and is taken into account in the code (see below) : the optical gain of the FEL is limited in space by the electron beam cross section, which RMS dimensions are close to 1 or 2mm. This influences the laser mode size in the undulator, as it induces a narrowing of the transverse profile of the laser.

In principle, the standard configuration for the cavity mirrors is a pair of spherical mirrors. However, at large wavelength, $\lambda > 50\mu\text{m}$ for CLIO, a better configuration is to use toroidal mirrors, which refocus the beam at the entry and output of the chamber in the vertical direction, whereas on the other axis, the free propagation requires the standard radius of curvature. Toroidal mirrors allows to lase at $\lambda > 100\mu\text{m}$ at CLIO. This toroidal configuration is used also such at FELIX and ELBE.

NUMERICAL CODE

The numerical code which has been used here [6] [7] [8] calculates the propagation of the laser wave front $A(x,y)$ in the optical cavity. It uses an iterative process of wave propagation in the cavity, which converges to a steady state laser mode, corresponding to the FEL saturation regime. It takes into account the design of the cavity (mirrors dimensions and radius of curvature), including the waveguide effect in the undulator section, and the hole coupling in the output mirror. The code uses a Gaussian transverse distribution of gain localized on FEL axis. Therefore, the maximum amplification of the laser wave is on axis. This will contribute to modify the waveguide mode distribution of the wave in the optical cavity.

This code gives the amplitude distribution $A(x,y)$ of the laser mode at saturation, in any point of the cavity and all related parameters : the cavity losses L , the extraction rate T_X of hole coupling, the intra-cavity laser power P_{in} and the output power P_{out} . The cavity losses are equal to $L = \Delta P_{in} / P_{in}$, where ΔP_{in} is the power loss of the intra-cavity laser pulse after one cavity round trip. The extraction rate $T_X = P_{out} / P_{in}$ is the ratio between output power P_{out} and intra-cavity power P_{in} . The calculation of all parameters : cavity losses, extraction rate and intensity at saturation, gives the FEL extracted power [8].

The calculation of the power at laser saturation is based on the theory of FEL intensity saturation which has been developed by G. Dattoli et al. [9] [10] [11]. The exponential gain takes into account the non linear Long Wavelength FELs

behaviour of Small Signal Gain in high gain regime, it includes the inhomogeneous broadning of filling factor and the longitudinal mode coupling factor. It is a single wavelength theory, which does not include short pulse effects of the FEL and is limited to narrow linewidth FEL operation. Also, the model does not take into account the shift of FEL resonance wavelength according to the waveguide mode number [12]. The relative frequency shift between the first and third order mode is approximately equal to : $[\lambda_R(q=3) - \lambda_R(q=1)] / \lambda_R = \lambda_R \cdot \lambda_o / b^2$, where λ_R is the resonance wavelength without waveguide, λ_o is the undulator period and b is the small dimension of the waveguide. For CLIO this means about 1% at 45 μm , so just within the bandwidth but for FELIX it is more than 3% at 53 μm . This means that the higher order modes necessarily must have a higher frequency in order to be amplified. Therefore, mode conversion in the free-space region could result in modes that are not amplified. However, it is likely that the 3rd order mode frequency is shifted at each pass toward the 1st one by the gain process and reaches a steady state. Our 2D programm does not take fully into account this effect, because it is a single frequency model, but the good agreement between simulations and experimental results show that this approximation is reasonable. Nevertheless, it may fail in the THz region where no data are available.

RESULTS FOR CLIO

Power measurements

We have measured the output laser power of CLIO as function of wavelength for various combinations of cavity mirrors. Wavelength tuning is made by undulator gap variation, whereas the electron beam energy is kept constant at 15MeV. These measurements have been recorded in a purged chamber in order to avoid laser absorption in air.

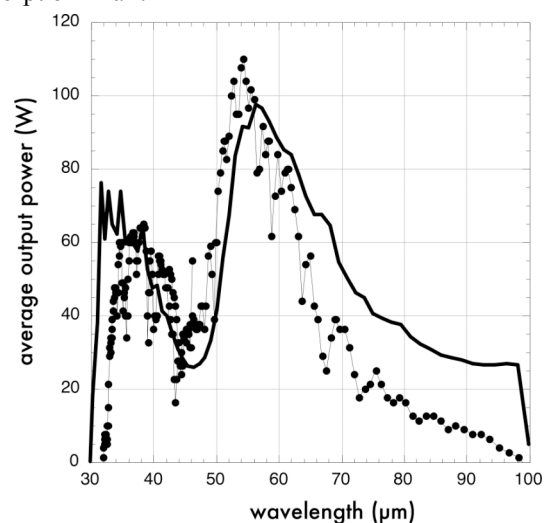


Figure 2 : laser power vs. centroid wavelength, for spherical mirrors cavity, using hole coupling of 2mm (dotted line : measurement, continuous line : simulation).

The first set of measurements is using spherical mirrors. A Spectral Gap appears at $\lambda=45\mu\text{m}$ and corresponds to a power decrease by a factor of about 2. The simulation fits very well measurements, including the absolute value of the power, with a realistic set of electron beam parameters : bunch charge $Q = 0.5 \text{ nC}$, energy spread $\sigma\gamma/\gamma = 0.5\%$, pulse length $\sigma_z = 4\text{ps}$, emittance $150 \mu\text{mm.mrd}$.

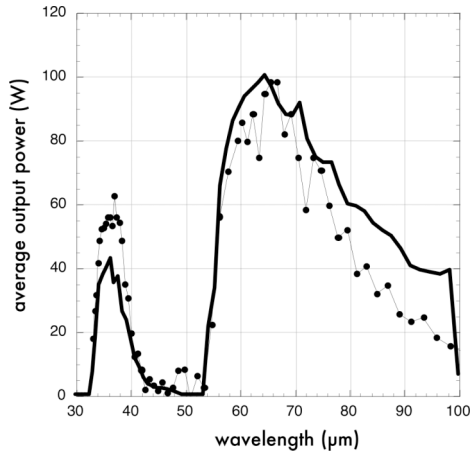


Figure 3 : laser power vs. centroid wavelength, for hybrid cavity : spherical for upstream and toroidal for downstream, using hole coupling of 3mm (bold line : simulation).

The figure 3 corresponds to a second set of measurements with an hybrid cavity, i.e. using a spherical upstream mirror and a toroidal downstream mirror. The Spectral Gap is more noticeable in this case. When using a full toroidal cavity, i.e. toroidal on both cavity mirrors, the Power Gap remains as shown in figure 4. These measurements show that Spectral Gaps are intrinsic effect, independant from optical cavity configuration.

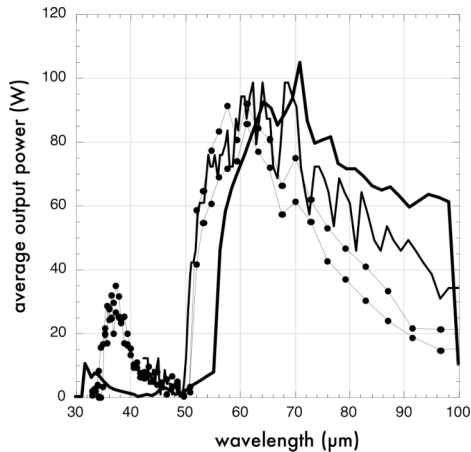


Figure 4 : laser power vs. centroid wavelength, for toroidal cavity, using hole coupling of 3mm (bold line : simulation).

Simulation for spherical cavity

In order to explain the Spectral Gap phenomenon, we used the numerical code to compute the cavity losses L and the hole coupling extraction rate T_X as a function of

Long Wavelength FELs

wavelength, and the laser mode profile at various places in the optical cavity. The figures 5 and 6 display them in the case of spherical mirrors cavity, i.e. related to power variations in figure 2.

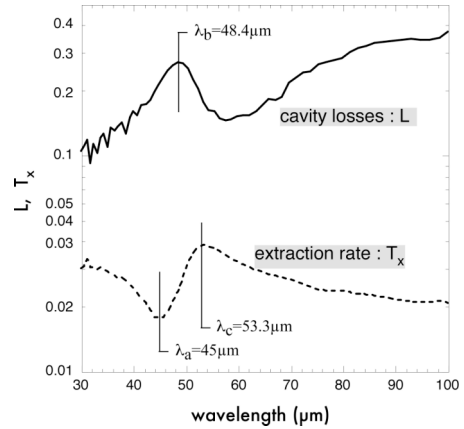


Figure 5 : Simulation of cavity losses L and hole coupling extraction rate T_X as a function of wavelength, for spherical cavity.

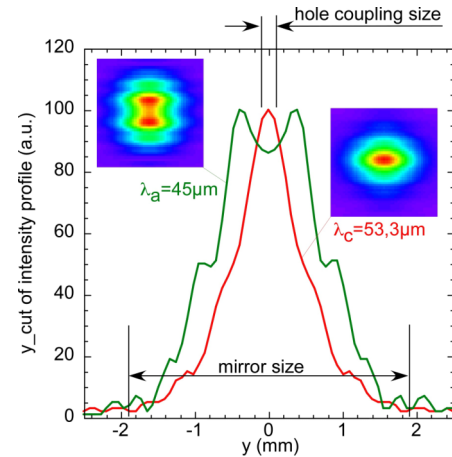


Figure 6(a) : Numerical simulation in the case of spherical cavity : laser mode transverse profiles on the output mirror, for 2 different wavelength.

The reason of the Spectral Gap is clearly visible : the extraction rate T_X exhibits a minimum at wavelength $\lambda_a=45\mu\text{m}$. The figure 6(a) displays the transverse profile of the laser mode, on the output mirror (point C in fig.1), for wavelengths λ_a and $\lambda_c=53.3\mu\text{m}$. At wavelength λ_a , the profile is wider and exhibits a small minimum of intensity in center, which accounts for the decrease of extraction rate T_X . This is a first reason which explains the output power decrease at $45\mu\text{m}$.

However, this is not the only cause of Spectral Gaps : despite of the lower extraction rate, the cavity losses are also maximum at wavelength $\lambda_b=48.4\mu\text{m}$. Mirror reflectivity is independent of wavelength, and Ohmic losses in the waveguide are negligible. A detailed analysis of the laser mode profile at the waveguide entrance, displayed in figure 6(b), shows that high losses in point λ_b are due to a broadening of the transverse size of laser mode, which does not fit the waveguide aperture. It

occurs only in the vertical plane, where the laser mode is guided.

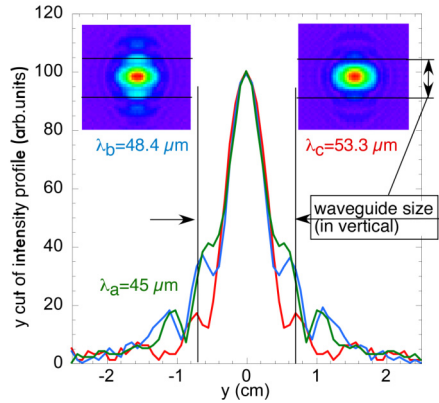


Figure 6(b): Numerical simulation in the case of spherical cavity: laser mode transverse profiles on downstream waveguide entrance (point B in fig.1), for 3 different wavelength.

At $\lambda_b=48.4\mu\text{m}$, about 20% of laser energy is lost at the two entrances of the waveguide. It represents only 8% at $\lambda_b=53.3\mu\text{m}$. This explains the peak of losses in the curve of figure 5, which is also responsible for the Spectral Gap observed in figure 2.

Simulation for toroidal cavity

As shown in figure 4, the Spectral Gap phenomenon with a toroidal cavity is even stronger than in the case of spherical cavity (figure 2). The figure 7 shows the cavity losses L , and the hole coupling extraction rate T_X , as a function of wavelength, for a toroidal cavity.

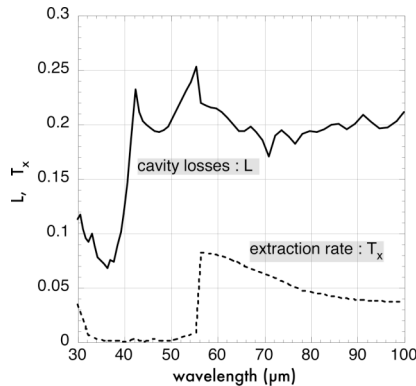


Figure 7: Simulation, total cavity losses L and hole coupling extraction rate T_X as a function of wavelength, for toroidal cavity.

The decreasing of the extraction rate T_X is much stronger here: there is a large range showing nearly zero extraction, between 32 and 55 μm . Also, within this range, the losses are varying strongly, and exhibit an important minimum at 37 μm . Such small losses are creating a large intra-cavity power P_{in} , as shown in figure 8 which displays both intra-cavity power P_{in} and output power P_{out} . The large value of P_{in} compensates partially the low extraction rate T_X , and leads to a significant output power P_{out} . This effect is shown in simulations

(fig.8), but it is even clearly observed in the measurements in figure 4.

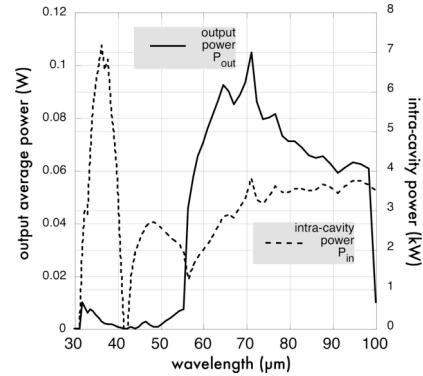


Figure 8: Simulation, output power P_{out} , and intracavity power P_{in} , as a function of wavelength, for toroidal cavity.

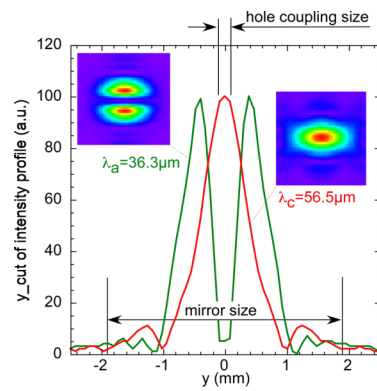


Figure 9(a): Numerical simulation in the case of toroidal cavity: laser mode transverse profiles on the output mirror, for two different wavelengths.

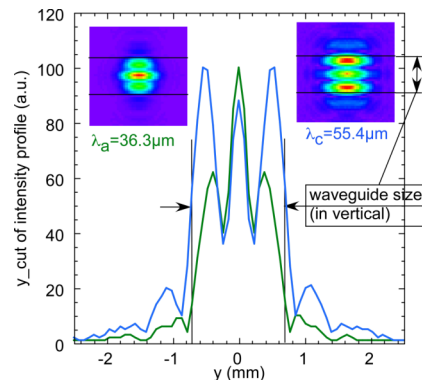


Figure 9(b): Numerical simulation in the case of toroidal cavity: laser mode transverse profiles on downstream waveguide entrance, for two different wavelengths.

In real experimental conditions, a small misalignment of cavity mirrors or of the electron beam allows the large intra-cavity power of the laser mode to be better outcoupled by the hole, than in the simulation. The Spectral Gap, which is observed here in the range 40 to 55 μm , is therefore due to the conjunction of a minimum of the extraction rate T_X with substantial cavity losses. The figure 9(a) displays the profiles on output mirror. The “two spots shape“ of the mode at 36.3 μm , explains the

low extraction rate T_X for $\lambda < 56 \mu\text{m}$. And the mode jumping, from 2 spots to 1 spot, between 55.4 and $56.5 \mu\text{m}$, explains the sharp variation of T_X at $56 \mu\text{m}$. Also, the strong minimum of cavity losses at $36.3 \mu\text{m}$ is due to the low extraction rate and the good fit of the mode profile into the waveguide aperture. Figure 9(b) displays the mode profiles at the downstream waveguide entrance (point B in fig.1). The sum of losses L at both entrances represents only 2.6% at $\lambda=36.3 \mu\text{m}$, which is rather low as compared to the other wavelengths.

RESULTS FOR OTHER INFRARED FELs

Results for FELIX

The optical cavity of the FELIX infrared FEL [4] is of same type as for CLIO, but with minor differences : the downstream cavity mirror is in contact with the waveguide, i.e. there is no free space between that mirror and the waveguide entrance. On the other hand, there is a free space of 1.66 m in front of the upstream mirror. The distance between cavity mirrors is 6 meters , and the waveguide length is 4.34 m , both of them are longer than CLIO. The figure 10 shows a comparison between simulation and measurement of the output power. Two measurements are displayed here : (1) for a perfect alignment of the cavity, and (2) for an alignment optimized at $\lambda=35 \mu\text{m}$. It shows that the Spectral Gap phenomenon exists on FELIX. The depth of Spectral Gaps may change with FEL alignment, but their positions remain identical.

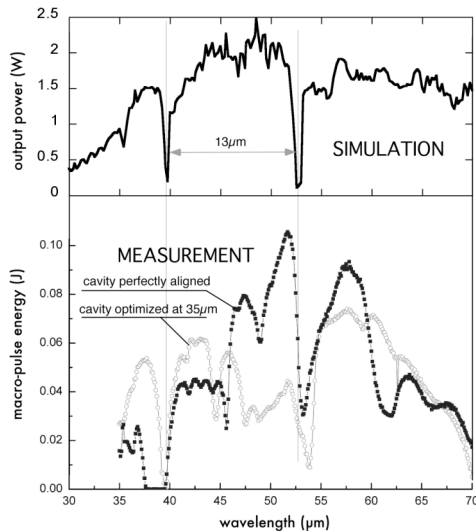


Figure 10 : Results for the FELIX infrared FEL.

The simulation exhibits the two main Spectral Gaps, at $38 \mu\text{m}$ and $53 \mu\text{m}$. We have done a detailed simulation around $\lambda=50 \mu\text{m}$, which is shown in figure 11. It displays P_{out} , P_{in} , L and T_X as a function of wavelength, and shows the mode profiles on output mirror (top images) and at waveguide entrance (bottom images). The main reason of the Spectral Gap at $53 \mu\text{m}$ is a minimum of extraction rate T_X : The “two spots shape” of the laser mode profile on

output mirror has a minimum of intensity on axis. On the other hand, the change of mode shape near $50 \mu\text{m}$ decreases cavity losses, inducing an increase of intracavity power P_{in} . However, this variation is dominated by the decrease of T_X in the calculation of the output power $P_{\text{out}}=T_X.P_{\text{in}}$. Note that for $\lambda=53.4 \mu\text{m}$, the mode exhibits a large transverse profile (in vertical), which does not fit the waveguide entrance. This explains the increase of the cavity losses.

As a summary, the Spectral Gap occurs at wavelengths corresponding to a jump of laser mode to a complex shape. Decreasing of output power occurs when the laser mode exhibits a “two spots shape” on the output mirror, which creates a decrease of the coupling T_X . This special mode is induced by the waveguide constraints. Indeed, we will see below that these constraints are depending on the dimensions of the waveguide.

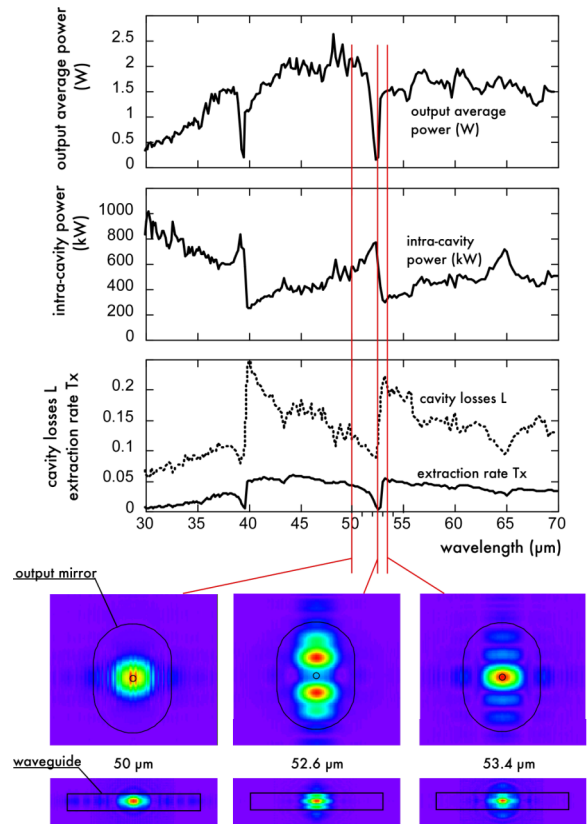


Figure 11 : Simulation for FELIX, with mode profiles on output mirror and at waveguide entrance, close to $\lambda=50 \mu\text{m}$.

Results for ‘ELBE’

The configuration of the U100 FEL, at ELBE laboratory in Forschungszentrum Dresden Rosendorf, Germany, is very similar to the FELIX FEL : the waveguide is in contact with downstream mirror. But the optical cavity is much larger, 11.5 meters long, and the waveguide also, 7.9 m . Figure 12 shows the result of the simulation, and displays the output power as a function of wavelength. Four Spectral Gaps are observed and they seem to be periodically spaced, with about a $7 \mu\text{m}$ period.

Unfortunately, the measurements of output power on ELBE are very lacunar, and they exhibit air absorption lines in the spectrum. Measurements in dry air environment are planned in the future.

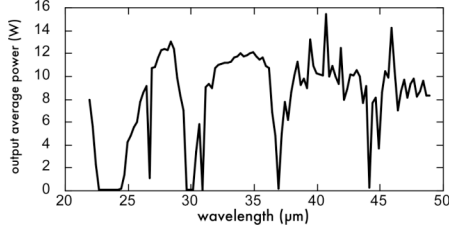


Figure 12 : simulation of output power on the U100 FEL in ELBE, at 32MeV, with 2mm hole coupling.

PHASE ANALYSIS IN THE WAVEGUIDE

The Spectral Gaps phenomenon is due to a particular combination of eigenmodes TE_q and TM_q , produced in the waveguide, which creates a mode profile producing large losses or low extraction rate. These eigenmodes are only vertically guided, because of the configuration of the waveguide (see above). Therefore the ‘p’ index of the modes is not used here. Though the numerical code does not use the eigenmodes to compute the wave propagation in waveguide section, we can deduce from the resulting profiles the energy distribution of the eigenmodes TE_q and TM_q in the waveguide. The figure 13 shows an example of this distribution in the case of CLIO at $\lambda=49.8 \mu\text{m}$, corresponding to a mode profile on output mirror with the two peaks structure as displayed in figure 9.

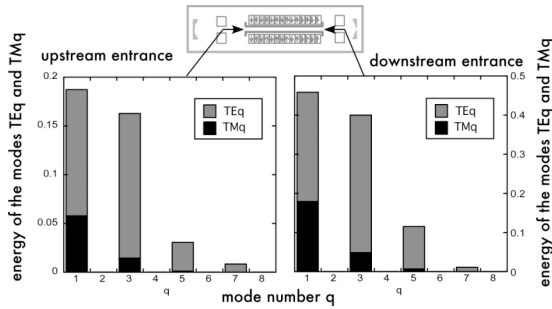


Figure 13 : energy distribution of eigenmodes on TE_q and TM_q in the case of CLIO, with toroidal mirrors, at $\lambda=49.8\mu\text{m}$.

Even modes are not present here, because they have a zero amplitude on axis and are not amplified by the electron beam which is centered on axis. This figure shows that the most important modes are $q=1$ and $q=3$.

It is likely that the phenomenon of Spectral Gaps is linked to the relative phase of the dominant cavity modes at the ends of the waveguide. Indeed, this phase will determine the diffraction losses at the entries of the waveguide and the mode structure at the extraction hole. Therefore, when sweeping the operating wavelength, one expects that a phase difference of 2π in a cavity roundtrip will account for the wavelength difference between two successive gaps.

The phase velocity in the waveguide for the mode q is :

$$v_q = \frac{c}{\sqrt{1 - \left(\frac{\lambda}{\lambda_c}\right)^2}} \equiv c \left(1 + \frac{\lambda^2 q^2}{8b^2}\right) \quad (1)$$

where $\lambda_c = 2b/q$ is the cut-off wavelength, and b is the waveguide aperture in vertical axis. The propagation time of mode q , in a waveguide of length L , is $t_q = L/v_q$. The relevant dephasing of mode q is :

$$\phi_q = \frac{2\pi}{T} t_q \equiv \frac{2\pi L}{\lambda} \left(1 - \frac{\lambda^2 q^2}{8b^2}\right) \quad (2)$$

the phase difference $\Delta\phi = \phi_1 - \phi_3$ between modes $q=1$ and $q=3$ is :

$$\Delta\phi = \phi_1 - \phi_3 = \frac{2\pi L \lambda}{b^2} \quad (3)$$

for a complete cavity round trip :

$$\Delta\phi_{RT} = \phi_1 - \phi_3 = \frac{4\pi L \lambda}{b^2} \quad (4)$$

This calculation does not make any hypothesis on the absolute phase distribution of the modes. It only gives the phase shift between mode 1 and mode 3, for one cavity round trip. Now, when choosing λ equal to the wavelength of a Spectral Gap, then the ‘next’ Spectral Gap in the FEL spectrum, at wavelength $\lambda' > \lambda$, must keep the same phase structure. This is the unique hypothesis that we do here : the phase structure is the same for all Spectral Gaps (for a given FEL configuration, of course). Therefore :

$$\text{for :} \quad \Delta\phi_{RT}(\lambda') = \Delta\phi_{RT}(\lambda) + 2\pi \quad (5)$$

one obtains :

$$\delta\lambda = \lambda' - \lambda = \frac{b^2}{2L} \quad (6)$$

where $\delta\lambda$ is expected to be the wavelength difference ($\lambda - \lambda'$) between two successive SG in the FEL power spectrum. Note that the 2π periodicity in expression (5) corresponds to a 4π periodicity when using upper modes $q=3$ and $q=5$. Therefore, as stated in the above hypothesis, the whole structure of modes TE_q and TM_q is kept constant between two consecutive Spectral Gaps at λ and λ' .

In order to check this simple analytical model, we show in figure 14 a simulation of FEL power as a function of wavelength, for various dimensions of waveguide aperture ‘ b ’. The parameters used in this calculation

correspond to the ELBE Free-electron laser, which the configuration gives the shorter wavelength period $\delta\lambda$.

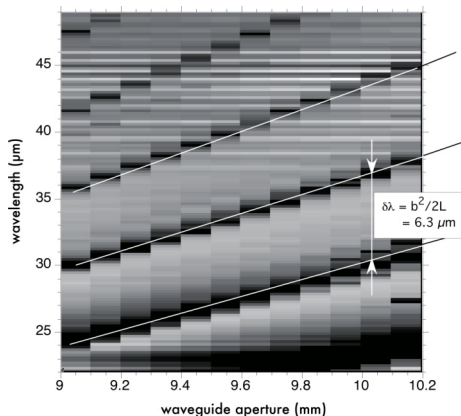


Figure 14 : simulation – ‘ELBE’ FEL power vs wavelength and waveguide aperture ‘b’.

Black lines correspond to Spectral Gaps, and the distance between two successive SG is $6.3 \mu\text{m}$ as predicted by the simple analytical expression (6) with $b=1\text{cm}$ and $L=7.92 \text{ m}$. Therefore, the simple model and the simulation agree very well, even if the available data do not allow to verify it experimentally.

Now for FELIX, the expression (6) gives $\delta\lambda=11.5 \mu\text{m}$, with $b=1 \text{ cm}$ and $L=4.34 \text{ m}$. The simulation curve in figure 10 shows that the distance between two successive SG is $\delta\lambda=13 \mu\text{m}$, which is not far from analytical and experimental values.

For the case of CLIO, the expression (6) gives $\delta\lambda=50 \mu\text{m}$. The first Spectral Gap in spectrum is measured at $\lambda=45$ to $50 \mu\text{m}$. Therefore, the next SG should be observed close to $\lambda=100 \mu\text{m}$, which is not the case. This could be explained by a further refinement of the above analytical model : one can assume that the gap occurs when the phase difference between mode 1 and 3 is $(2n + 1)\pi$, with n integer, along one pass in the waveguide. Indeed, if the phase between the 2 modes is such that the electric fields add at the center of the chamber and subtract on the sides, the intensity profile will exhibit the smallest possible spatial width, thus minimizing diffraction losses. Also, the profile peaking at the center will favor laser power extraction by the outcoupling hole. If the phase difference along the chamber is $2n\pi$, one gets the same profile at each end, which is the more desirable situation and if it is $(2n+1)\pi$, it is the most disadvantageous one, giving rise to the Spectral Gap. Expression (6) becomes then :

$$\lambda = \frac{b^2}{2L}(2n + 1) \quad (7)$$

This accounts for the position of the first gap, then at $50 \mu\text{m}$ on CLIO, as observed, and the second should be at $150 \mu\text{m}$, where diffraction losses are too large to obtain lasing. At FELIX and ELBE, one side of the waveguide is in contact with one of the cavity mirror, so that the

effective length of the waveguide is doubled and eq. (6) becomes :

$$\lambda = \frac{b^2}{4L}(2n + 1) = \frac{b^2}{2L}\left(n + \frac{1}{2}\right) \quad (8)$$

The periodicity remains unchanged and the first gap is situated at a short wavelength ($< 10 \mu\text{m}$) where no waveguiding occurs. The conditions expressed in (7) and (8) are compatible with eq. (6), they are only more restrictive.

This explanation is not fully quantitative, as already mentioned above. In particular, it does not explain the "violent" character of the increase of the losses in the vicinity of the spectral gap. As can be seen on fig. 11, the optical mode shape exhibit two peaks only in a short wavelength interval around the one where the minimum power occurs. This is due to fast variations in the content of waveguide modes, not taken into account in the simple analytic model but only in the simulations.

Nevertheless, the above expressions provide an order of magnitude of the number N_{SG} of Spectral Gap in a given FEL spectral range, proportionnal to L/b^2 . In an apparent paradox, this number becomes larger for a longer waveguide and is of the order of more than 10 in the wavelength range of ELBE.

CONCLUSION

The Spectral Gap phenomenon has been observed on various infrared FELs. This phenomenon produces a series of holes in the tuning range of the FELs using partial waveguiding of the light, in order to alleviate diffraction losses in far infrared. It is unavoidable and depends only on the characteristics of the waveguide used. The explanation of Spectral Gap phenomenon is quite complex, because it is dependant on two independant parameters : (1) hole coupling extraction rate, and (2) optical losses in waveguide entrance. Both of them, are strongly dependant on slight variations of the transverse mode profile. Also, they can be somewhat uncorrelated, as shown in figure 7, leading to large differences in the behavior of the gaps. As a consequence, a simple analytical model, described above, only gives an order of magnitude of the expected number of Spectral Gaps in the FEL range. A detailed analysis requires the simulation code, which results are in rather good agreement with measurements.

We have shown here that the number of Spectral Gaps is proportional to the waveguide length and to $1/b^2$, where b is its width. In the typical tuning range of an infrared FEL the number of gaps can be quite large. This is a very penalizing problem for a FEL, which main virtue is normally its large range of tunability. This must be taken into account in the engineering of future far-infrared FELs using partial waveguiding in the optical cavity.

ACKNOWLEDGEMENTS

We are thankful to Lex van der Meer, and more generally to the FELIX free-electron laser group, for their contribution by sending us experimental data for the FEL. Thanks also to Wolfgang Seidel from the ELBE free-electron laser for sending data from the FEL.

REFERENCES

- [1] M. E. Couprie and J. M. Ortega, "Free-electron lasers sources for scientific applications", *Analisis*, 28, 725 (2000)
- [2] J.M.Ortega, F.Glotin, R.Prazeres, "Extension in far-infrared of the CLIO free-electron laser", *Infrared Physics and Technology*, 49, 133 (2006)
- [3] R. Prazeres, F. Glotin, J.M. Ortega, 'New results of the CLIO infrared FEL', *Nucl. Instr. & Meth. A528* (2004) 83-87
http://clio.lcp.u-psud.fr/clio_eng/clio_eng.htm
- [4] Li Yi Lin, A.F.G. van der Meer, "Design of a short-pulse, far-infrared free electron laser with a highly overmoded waveguide", *Rev. Sci. Instrum.* 68 (1997) 4342-4347.
http://www.rijnhuizen.nl/research/guthz/felix_felice
- [5] P.Michel et al., "The Rossendorf IR-FEL ELBE", proceedings FEL 2006 – BESSY, Berlin, Germany, p488-491
<http://cern.ch/AccelConf/f06/PAPERS/TUCAU02.PDF>
- [6] R. Prazeres, V. Serriere, "Calculation of intracavity laser modes in the case of a partial waveguiding in the vacuum chamber of the CLIO FEL", *Nucl. Instr. And Meth. A* 475, 524-530 (2001)
- [7] R.Prazeres, "A method of calculating the propagation of electromagnetic fields both in waveguides and in free space, using the Fast Fourier Transform", *Eur. Phys. J AP* 16, 209-215 (2001)
- [8] R.Prazeres, F.Glotin, J.M.Ortega, "Measurement and calculation of the Electron efficiency on the CLIO Free-Electron Laser", *Eur. Phys. J. Appl. Phys.* 29, 223-230 (2005)
- [9] G.Dattoli, "Logistic function and evolution of free-electron-laser oscillators", *Jou. of Appl. Physics*, 84, (1998) p2393-2398
- [10] G.Dattoli, PL.Ottaviani, "Semi-analytical models of free electron laser saturation", *Optics Com.* 204 (2002) 283-297
- [11] G.Dattoli, T.Letardi, JMJ.Madey, A.Renieri, "Single passage FEL devices: A preliminary comparison with conventional coherent sources", *Nucl.Instr.& Methods A237* (1985) 326-334
- [12] J.W.J. Verschuur, G.J. Ernst, B.M. van Oerle, D. Bisero, "The effect of transverse modes in a waveguide resonator on the resonance condition of a Compton FEL", *Optics Communication*, 133, (1997) p229-233